1994A&AS..107...29S

ASTRONOMY & ASTROPHYSICS
SUPPLEMENT SERIES

Astron. Astrophys. Suppl. Ser. **107,** 29-38 (1994)

Atomic data from the IRON project. IV. Electron excitation of the $^2P^\circ_{3/2}$–$^2P^\circ_{1/2}$ fine structure transition in fluorine-like ions

H.E. Saraph[1] and J.A. Tully[2]

[1] Department of Physics and Astronomy, University College London, London WC1E 6BT, U.K.
[2] URA 1362 du CNRS, Observatoire de la Côte d'Azur, BP 229, 06304 Nice Cedex 4, France

Received October 18, 1993; accepted April 13, 1994

Abstract. — Total collision strengths for the ground term fine structure transition in 17 fluorine-like ions from Ne II to Fe XVIII are obtained in the close coupling approximation. Model target ions with only two terms, $2p^5\,^2P^\circ$ and $2s2p^6\,^2S$ are used, so that the collision strengths are perturbed by autoionizing resonances which converge on the excited ^2S term. These features are carefully delineated before averaging over a Maxwell velocity distribution to obtain effective collision strengths. The thermally averaged collision strengths should be reliable for the infrared lines excited at low temperatures in astrophysical situations where photoabsorption dominates the ionization equilibrium. The present calculation ignores resonances which converge on terms that lie above ^2S. These are expected to make a significant contribution to the collision rates at higher temperatures. We give the range of temperatures where the present results should be reliable.

Key words: atomic data — infrared: general

1. Introduction

The Infrared Space Observatory (ISO) will be able to detect infrared lines ($\lambda > 1$ μm) from many atomic species. Reliable collision rates are essential for interpreting these observations. Ions at the beginning of the fluorine sequence are possible emitters of infrared lines since their ground configuration $2p^5$ gives rise to two fine structure levels whose separation corresponds to wavelengths in the range 12.7 μm (Ne II) to 1.37 μm (P VII). The present investigation was initially motivated by the demands for data for ISO and is part of an international collaboration known as the IRON Project (see Hummer et al. 1993, to be referred to as Paper I). A number of scattering calculations have been completed for individual ions of the fluorine sequence, see the review by Bhatia (1994). The ions that have been treated with very elaborate target state expansions are Ne II (Johnson & Kingston 1987), Mg IV (Johnson & Kingston 1987 and Mendoza & Zeippen 1987), Si VI (Mohan & Le Dourneuf 1990), Fe XVIII (Mohan et al. 1987) and Ni XX (Mohan et al. 1990). Most of the earlier work is not presented in a way that accurate collision rates can be extracted, as will be discussed in Sect. 4. It is the policy of the IRON Project to treat complete isoelectronic sequences up to iron initially with relatively simple collision targets, in order to generate a useful data base, and then to select ions that indicate special problems for an elaborate and very detailed investigation. In this paper a simple target that gives collision strengths valid at low energies is used. Particular emphasis is placed on the establishment of accurate methods for the calculation of thermally averaged collision strengths.

The two-state target is described in Sect. 2, Sect. 3 gives details of the scattering calculation, Sect. 4 discusses the problems associated with thermal averaging when the collision strengths contain series of resonances and Sect. 5 discusses the results and their limitations.

2. Target wave functions for fluorine-like ions

Hibbert & Scott (1994) devised a simple but satisfactory two-state target based on the single configuration orbitals calculated by Clementi & Roetti, (1974). They used configuration interaction (CI) representations including a non-spectroscopic orbital $\bar{3}$d. The single exponent for the Slater type $\bar{3}$d orbital was determined so as to minimise the ground state energy. The two target terms are represented by the configurations
$^2P^\circ$: $1s^22s^22p^5$, $1s^22s2p^5(^1P,^3P)\bar{3}d$ and
^2S: $1s^22s2p^6$, $1s^22s^22p^4(^1D)\bar{3}d$.
The exponents for the $\bar{3}$d orbitals obtained by Hibbert and Scott vary smoothly along the sequence except for

© European Southern Observatory • Provided by the NASA Astrophysics Data System

1994A&AS..107...29S

Z=10 for which we used our own optimised value. Whilst those authors considered only ions with nuclear charge Z = 10 ... 14, 16, 20 and 26, we require orbitals for all ions with Z = 10 ... 26 and have used spline interpolation to find the missing exponents for the $\bar{3}$d orbitals; the fit was excellent with a rms deviation of only 0.04%. The resulting values are shown in Table 1. These are used in our collision calculations. For some of the ions the data were checked using the program CIV3 by Hibbert (1975).

In Table 2 relevant information about the target states is provided. We give the theoretical and experimental ^{2}P° – ^{2}S term separations, $E_{\rm th}$ and $E_{\rm ex}$, the latter is calculated with respect to the centre of gravity of ^{2}P°. They agree quite well. Next we give the calculated oscillator strengths in the length and velocity formulations. Their good agreement indicates that the CI representation of the two terms is well balanced. Mohan & Hibbert (1991) have calculated oscillator strengths for some fluorine-like ions with a much more elaborate CI expansion. We include their values in Table 2; the agreement is satisfactory. In conclusion, one may have confidence in using these targets in the scattering calculations. Table 2 also gives the ^{2}P° fine structure splitting and the estimated energies at which the onset of resonances from terms that have been neglected in this calculation must be expected. The significance of these two columns is discussed in Sects. 4 and 5. Rydberg units are used throughout this paper. References to the sources of experimental data for the various ions are listed in Table 3.

3. The scattering calculation

The basic atomic theory, the approximations and the computer codes employed in the IRON Project are described in Paper I. The scattering calculations were carried out in *LS* coupling. Collision strengths for fine structure transitions were obtained using an algebraic transformation to intermediate coupling, as described in Sect. 2.6 of Paper I. This procedure makes no allowance for the fine structure splitting of the term ^{2}P°. Possible effects are discussed in Sect. 5.

In the codes used here, only the dipole and quadrupole parts of the potential are taken into account in the asymptotic region. That this was adequate for optically forbidden fine structure transitions was confirmed by comparison with calculations using a program by Vo Ky Lan (1991), that includes all orders of the multipole expansion of the potential.

Experimental target energies are available for all ions. Their use is crucial for correcting the positions of resonance states $2s2p^6(^2S)\nu l$ relative to ^{2}P° for Z=13, 15 and Z>16, where some resonances lie close to the excitation threshold. Such near-threshold resonances have a large effect on the low temperature collision rates.

Accurate determination of collision rates depends on adequate tabulation of the collision strengths. Care was taken to delineate all resonances by using a tabulation grid $\delta\nu = 0.002$ rather than constant energy mesh for the interval $\nu = \nu_{\rm thr}$ to $\nu = \nu_{\rm thr}$+3.5 or to ν=6.2 whichever is the larger. Table 4 lists effective quantum numbers $\nu_{\rm thr}$ with respect to ^{2}S

$$\nu_{\rm thr} = (Z-9)/[E(^2{\rm S}) - E(^2{\rm P}^\circ_{\rm cg})]^{1/2}$$

at the excitation threshold for the ^{2}P° fine structure transition. This column also indicates the progression of members of the $2s2p^6(^2S)\nu l$ Rydberg series from continuum to bound states as Z increases. The next three columns of Table 4 list the effective quantum numbers of a 3s, 3d and 3p electron respectively. One observes the typical decrease of quantum defects as Z increases. Correspondingly, the resonances associated with a given principal quantum number all crowd together for high Z, as can be seen in Fig. 1, that illustrates the collision strengths for the sequence. Using the data given in Table 4 all resonances shown in Fig. 1 can be identified. The effective quantum number ν(3p) can be compared with experimental values for most ions, see the last column of Table 4. The agreement is very satisfactory, which indicates good accuracy of the scattering calculation. As the electron energy approaches the ^{2}S threshold from below the widths of the resonance structures become narrow compared to that of the electron velocity distribution. At these energies, the most accurate procedure for the purpose of calculating collision rates is to obtain collision strengths that have been averaged over the resonance structure. As is clearly seen in Fig. 1 the averaged collision strength is about a factor 2 larger than the background value between the resonances and the value above the ^{2}S threshold. The formulation for this 'Gailitis average' was derived by Seaton (1983) using quantum defect theory and is employed in the present codes, see Paper I. For Ne II and Mg IV we can compare the present calculation with the two-state calculations of Johnson & Kingston (1987) who use much more elaborate target wave functions and who also delineate the resonances very carefully. We note that our resonance positions are slightly shifted, especially for Ne II, where Johnson and Kingston agree better with experiment. For Mg IV the differences are negligible. For both ions the results by Johnson and Kingston are superior to those from the present calculations.

4. The effect of resonances on the accuracy of the collision rates

In this paper we are concerned only with resonances due to quasi-bound states of configuration $1s^22s2p^6(^2S)\nu l$ that occur at energies

$$E_{\rm res} = -\frac{(Z-9)^2}{\nu^2} \qquad (1)$$

relative to ^{2}S. The transition ^{2}P° – ^{2}S is optically allowed, whilst the fine structure transition $^2{\rm P}^\circ_{3/2}$ – $^2{\rm P}^\circ_{1/2}$

© European Southern Observatory • Provided by the NASA Astrophysics Data System

1994A&AS..107...29S

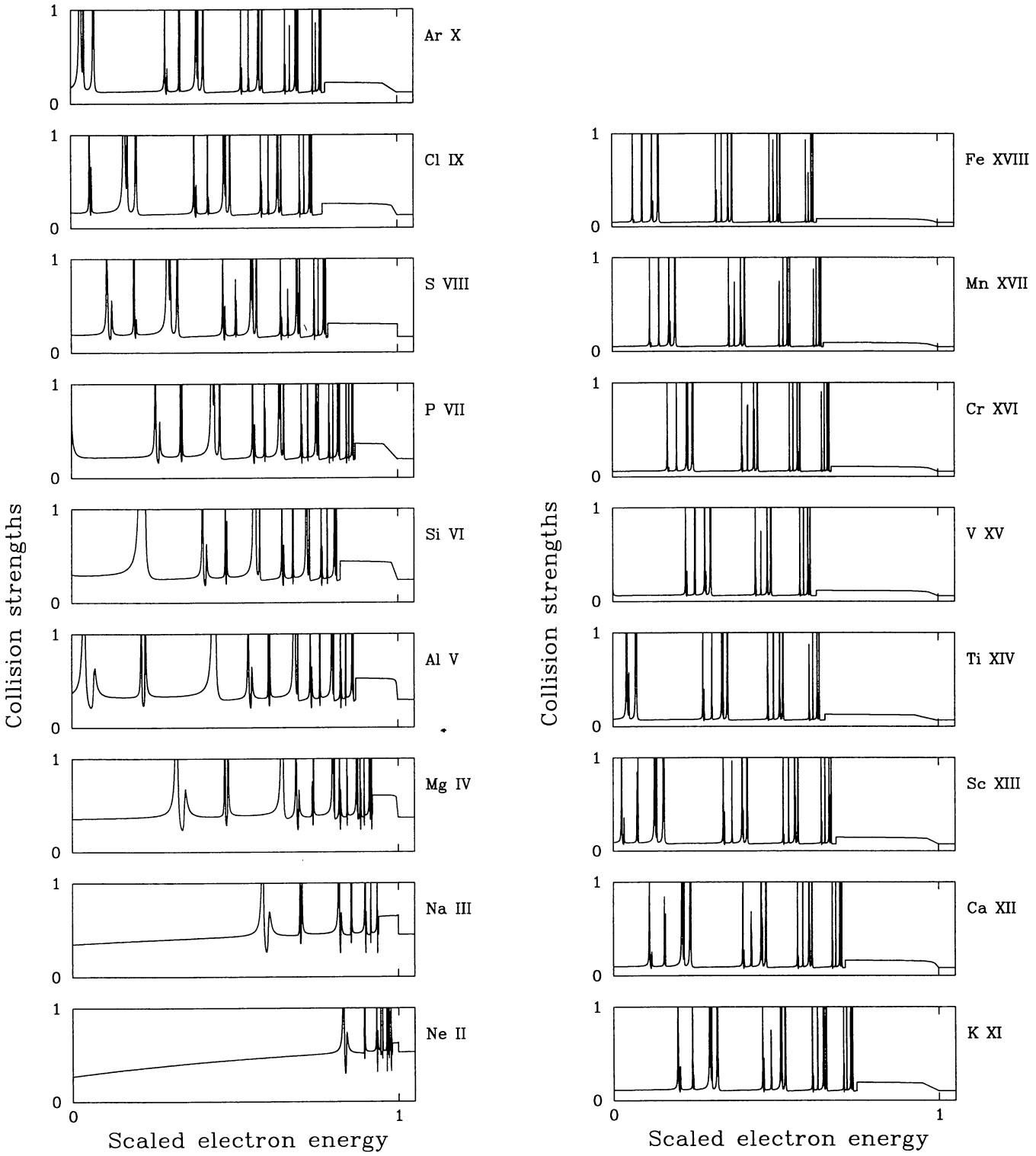

Fig. 1. Collision strengths Ω ($^2P^o_{3/2} - ^2P^o_{1/2}$) for fluorine - like ions with Z= 10 ... 26. 'Scaled electron energy" is the collision energy divided by $E(^2P^o - ^2S)$

© European Southern Observatory • Provided by the NASA Astrophysics Data System

1994A&AS..107...29S

that we are studying is optically forbidden. Consequently the resonances have a dominant effect on the fine structure collision strengths below the ^{2}S threshold. The thermally averaged or 'effective' collision strength Υ is defined by

$$\Upsilon_{if}(T) = \int_0^\infty \Omega_{if}(\epsilon) \mathrm{e}^{-\epsilon/kT} \mathrm{d}(\epsilon/kT), \qquad (2)$$

where k is the Boltzmann constant, ϵ is the electron energy in Rydberg units relative to the centre of gravity of ^{2}P°, T is the temperature in Kelvin and Ω is the collision strength. The excitation rate coefficient q_{fi} is obtained from

$$q_{fi} = \frac{8.6287\ 10^{-6}}{w_i T^{1/2}} \Upsilon_{if}(T) \mathrm{e}^{-E_{\mathrm{FS}}/kT} \quad \mathrm{cm}^3\mathrm{s}^{-1}, \qquad (3)$$

where w_i is the statistical weight of the lower level (^{2}P°$_{3/2}$) and E_{FS} is the finestructure energy tabulated in Table 2. The procedure of thermal averaging, using the Maxwell velocity distribution for a given electron temperature T, heavily weights the collision strengths at the corresponding energies. It is therefore essential to calculate the shapes and positions of the resonances to the best possible accuracy. We have to consider four sources of errors.

i) *The calculated energy difference* ^{2}P°$-$ ^{2}S *does not correspond to observations.* It is possible to compensate for this discrepancy by introducing the experimental energy differences as stated in Sect. 3. This ensures that the energies of resonances due to Rydberg series converging on the ^{2}S target state have the correct position relative to the centre of gravity of the ground term ^{2}P°.

ii) *The potential seen by the electron impinging on the model ion differs from that of the genuine ion.* As a result the scattering phase is somewhat incorrect. The effective quantum number of a bound or quasi bound state is similarly affected, so that resonances are not quite in the correct position. In Table 4 effective quantum numbers for states 2s2p^6(^{2}S)3p ^{1}P° are given and compared with experiment. As the differences are quite small this source of error will be relatively insignificant.

iii) *The effects of higher target terms are neglected in the present calculation.* We have looked for calculations that include higher target states. Mendoza & Zeippen (1987) use a five-state target expansion for Mg IV. They find that the thermally averaged collision strength is nearly constant and they give Υ=0.358 for temperatures around 20000 K. This is in excellent agreement with our results. Mohan & Le Dourneuf (1990) have calculated the collision strength for Si VI with a very elaborate target state expansion. In Fig. 2a,b we compare the results for Si VI of Mohan and Le Dourneuf with the present calculation. It is seen that at low energies our results match theirs quite accurately. As the energy increases the resonance pattern obtained by Mohan and Le Dourneuf, Fig. 2a, shows less detail and less repetitiveness than ours, but still the same number of resonances and the same background collision strength. At 3.1 Ryd we start to use the Gailitis average and our graph, Fig. 2b, does not show any more resonances. Mohan et al. (1987) give low energy collision strengths for Fe XVIII, using a 13-state target expansion. Again, the background collision strength and the resonance positions agree very well with our calculation. The energy for the onset of resonances due to higher target terms can be estimated reliably from the experimental energy of the next higher target term, 2s^{2}2p^4(^{3}P)3s ^{4}P, and the effective quantum number of a 3s electron, using Eq. (1) and ν(3s) of Table 4. The configuration of the lowest resonance state that we neglect is 2s^{2}2p^{4}3s^2. We give the estimated energies of these states, E_{L}, in Table 2. These energies limit the validity range of our results and indeed any other calculation that includes only two target states. The comparison with Mohan and Le Dourneuf and with Mohan et al. shows that the higher target terms that they include do not affect the background cross section nor the resonance pattern at energies below E_{L}.

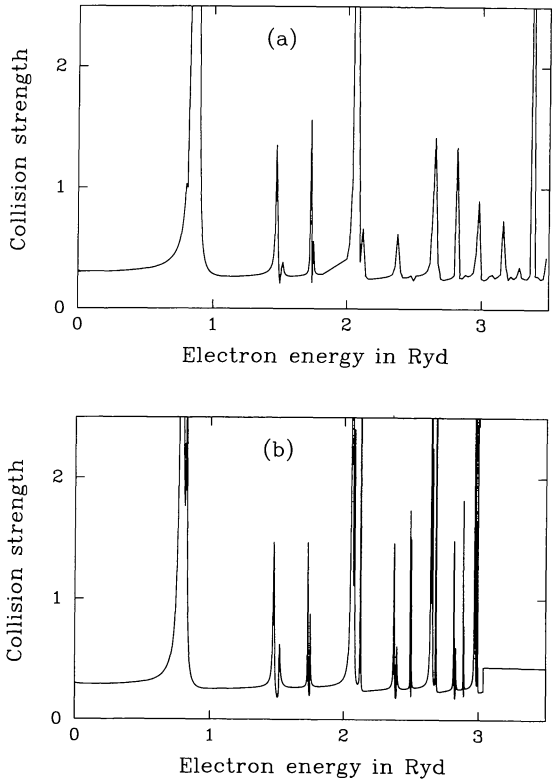

Fig. 2. Fine structure collision strengths $\Omega(^2\mathrm{P}^\circ_{3/2} - ^2\mathrm{P}^\circ_{1/2})$ for Si VI. a) Mohan & Le Dourneuf 1990. b) present work

iv) *The fine structure splitting of* ^{2}P° *is neglected.* A calculation in *LS* coupling ignores all fine structure splitting. This affects the relative position of the excitation threshold to the resonances, and is significant for high Z ions where there are resonances close to the excitation threshold. We have examined this source of error; it is further discussed in Sect. 5.

© European Southern Observatory • Provided by the NASA Astrophysics Data System

1994A&AS..107...29S

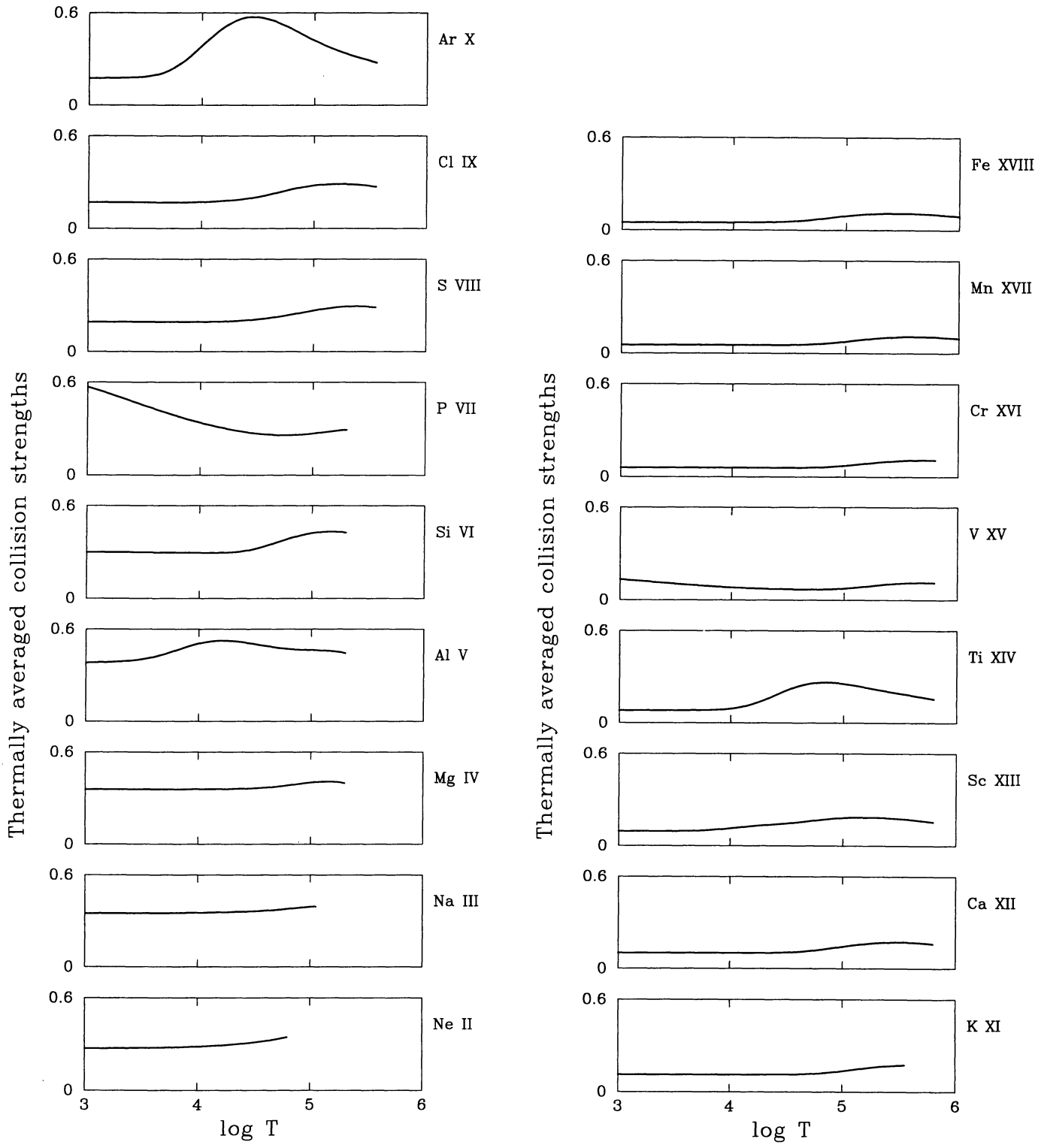

Fig. 3. Thermally averaged collision strenghts $\Upsilon(^2P^o_{3/2} -^2 P^o_{1/2})$ for fluorine - like ions with Z= 10 ... 26

© European Southern Observatory • Provided by the NASA Astrophysics Data System

1994A&AS..107...29S

5. Results and discussion

Thermal averaging is carried out by applying linear interpolation to the tabulated values of the collision strength followed by analytical integration as described by Burgess & Tully (1992). The thermally averaged collision strengths $\Upsilon(T)$ are presented in Table 5 and in Fig. 3. Results for Ne II and Mg IV can be compared with the more elaborate two-state calculations by Johnson & Kingston 1987. They differ by less than 8% for Ne II and by less than 4% for Mg IV. Entries in Table 5 are restricted to temperatures and ions where the present calculations are considered reliable. Figure 3 illustrates that the thermally averaged collision strengths show a highly diverse behaviour along the isoelectronic sequence. This is due to the sensitivity of the thermal averaging to the resonance pattern, which in turn shifts systematically to lower energies as Z increases, see Fig. 1. For $Z = 13$, 15, 18, 21, 22 and 26 one finds resonances at the excitation threshold and correspondingly an increase in the effective collision strength. For scandinavium, Z=21, the effect is small because the resonances in question, $2s2p^6(^2S)5s$ are narrow and have relatively small peak values. For titanium, Z=22, the effect is enormous because the contributing resonances, $2s2p^6(^2S)5d$, 5f, and 5g, are broadened through overlap and have peak values that are two orders of magnitude higher than the background collision strength. Considering the sensitivity of thermal averaging to the positions and shapes of the resonances we have been careful to reduce errors that could affect these. As indicated in Sect. 2 the target state representation is satisfactory. As described in Sect. 3 collision strengths in the region of resonances converging on ^2S were accurately delineated, and close to the ^2S threshold an average over the resonances was obtained. Experimental energies were used to replace the theoretical term energies for ions with Z=13, 15 and $Z > 16$. We illustrate the effect of this replacement with the following example. Figures 4a,b give the collision strengths for Ar X using theoretical and experimental target term separations respectively, and Fig. 5 shows the corresponding thermally averaged collision strengths Υ. Although the collision strengths look almost identical, the differences between the effective collision strengths are quite dramatic, due to the large 4d resonance just above the excitation threshold.

The fact that we only use a two-state ion model limits the range of energies at which our results are strictly valid. At higher energies the results of Mohan & Le Dourneuf (1990) and of Mohan et al. (1987) indicate a steep rise in the effective collision strength that is due to resonances converging on higher target states. Unfortunately we can not recommend the results of Mohan and Le Dourneuf because their tabulation grid is inadequate for reliable thermal averaging. Where Fig. 2b shows distinct narrow spikes and a repetitive pattern, their graph, Fig. 2a, shows irregular broad based triangles. Correspondingly, their effective collision strength is overestimated. Mohan et al. (1987) start tabulating their effective collision strength for Fe XVIII at 10^6 K. At this temperature our result for the effective collision strength, 0.0930, agrees well with theirs, 0.0905. At higher temperatures their effective collision strength increases rapidly.

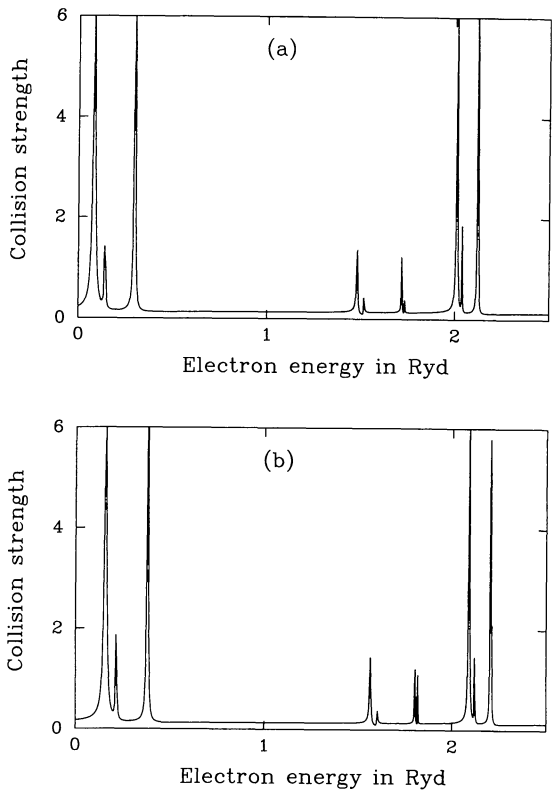

Fig. 4. Collision strengths $\Omega(^2P^\circ_{3/2} - ^2P^\circ_{1/2})$ for Ar X. a) using the calculated term separation $E_{\rm th}(^2P^\circ - ^2S)$; b) using the experimental term separation $E_{\rm ex}(^2P^\circ_{cg} - ^2S)$

We still have to consider errors due to the use of the *LS* coupling representation. The fine structure splitting of the $^2P^\circ$ term is neglected and its centre of gravity is used when replacing calculated by 'experimental' term separations in the codes. With increasing Z the splitting becomes large compared to the widths of the resonances near the excitation threshold. Where a group of resonances straddles the threshold our results become unreliable at low temperatures. The ions affected in this way are Ar X, Ti XIV, Mn XVII and Fe XVIII. The only satisfactory solution to this problem is a fully relativistic calculation. This is presently being carried out for Fe XVIII by Berrington (1993). One can expect that the positions of the resonances will not shift significantly in such a calculation because the relativistic part of the potential does not affect the high-lying quasi-bound states very much. One may thus mimic the effect of the fine structure splitting by using electron energies $\epsilon_a = \epsilon - [E(^2P^\circ_{\frac{1}{2}}) - E(^2P^\circ_{cg})]$ in place of ϵ in Eq. (2) and starting the integration at $\epsilon_a = 0$.

© European Southern Observatory • Provided by the NASA Astrophysics Data System

1994A&AS..107...29S

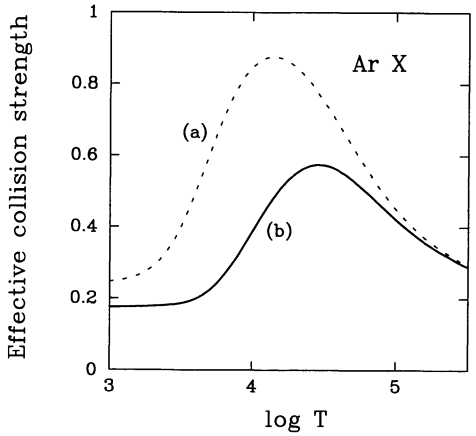

Fig. 5. Thermally averaged collision strengths $\Upsilon(^2P^o_{3/2} - {}^2P^o_{1/2})$ for Ar X. Full line: experimental term separation; dotted line: theoretical term separation

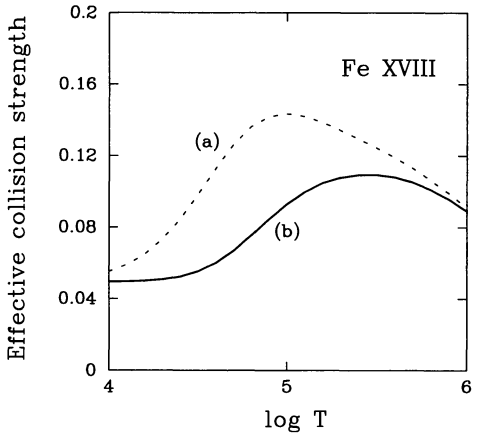

Fig. 6. Thermally averaged collision strenghts $\Upsilon(^2P^o_{3/2} - {}^2P^o_{1/2})$ for Fe XVIII. a) adjusted so as to mimic the use of the experimental level separation $E(^2P^o_{1/2} - {}^2S)$; b) using the experimental term separation $E_{ex}(^2P^o_{cg} - {}^2S)$

In Table 6 we present such empirically adjusted Υ_a for Ar X, Ti XIV, Mn XVII and Fe XVIII alongside those Υ obtained as in Table 5. For these ions the differences are rather large at low temperatures. We show Υ and Υ_a for Fe XVIII in Fig. 6. The effective collision strengths differ over a wide range of temperatures but this poses no serious problem because the abundance of Fe XVIII for this range of temperatures is low. Results of a relativistic calculation in the Breit-Pauli approximation, using the same target wave functions as in the present calculation, have already been given in paper I for Fe XVIII. We quote the results in Table 6 and it is seen that Υ_a and Υ_{BP} agree very well. This gives us some confidence in our procedure for empirically adjusting the effective collision strengths. Whilst fully relativistic calculations are not available, we recommend the Υ_a of Table 6, but stress that low temperature results for Ar X and Ti XIV are of poor accuracy. We have tested the effects of the fine structure splitting on all ions with $Z > 17$ and are satisfied that the results given in Table 5 would not change by more than 10% at any temperature.

As we have shown there are unresolved difficulties that affect certain low temperature and high temperature results. Therefore extrapolations of the effective collision strengths given in Tables 5 and 6 are not reliable.

For the heavy ions in the sequence, fully relativistic calculations exist using the distorted wave approximation, Sampson et al. (1991). Unfortunately, that approximation does not include the resonance effects that are found to be so important. For background values and for high energies the present collision strengths agree quite well with those calculations, as is shown in Table 7. At very high energies the results by Sampson et al. should be reliable.

Acknowledgements. We would like to thank David Hummer for his helpful comments on the original draft of this paper. The project has been supported by SERC grant GR/H/94979. The figures in this article were drawn using the graphics package 'Tout Va Bien' developed by Georges Gonczi at Nice Observatory. We are grateful to him for providing us with a copy and for his friendly guidance.

References

Berrington K.A. 1993, private communication
Bhatia A.K. 1994, At. Data Nuc. Data Tables 57, 253
Burgess A. and Tully J.A. 1992, A&A 254, 436
Clementi E. and Roetti C. 1974, At. Data Nuc. Data Tables 14, 177
Corliss C. and Sugar J. 1977, J. Phys. Chem. Ref. Data 6, 1253
Corliss C. and Sugar J. 1979, J. Phys. Chem. Ref. Data 8, 1
Corliss C. and Sugar J. 1982, J. Phys. Chem. Ref. Data 11, 135
Deutschman W.A. and House L.L. 1966, ApJ 144, 435
Hibbert A. 1975, Computer Phys. Commun. 9, 141
Hibbert A. and Scott P., 1994, J. Phys. B: At. Molec. Opt. Phys. 27, 1315
Hummer D.G., Berrington K.A., Eissner W. et al. 1993, A&A 279, 289
Johnson C.T. and Kingston A.E. 1987, J. Phys. B: At. Mol. Phys. 20, 5757
Martin W.C. and Zalubas R. 1979, J. Phys. Chem. Ref. Data 8, 817
Martin W.C. and Zalubas R. 1980, J. Phys. Chem. Ref. Data 9, 1
Martin W.C. and Zalubas R. 1981, J. Phys. Chem. Ref. Data 10, 153
Martin W.C. and Zalubas R. 1983, J. Phys. Chem. Ref. Data 12, 323
Mendoza C. and Zeippen C.J. 1987, MNRAS 224, 7p
Mohan M., Baluja K.L., Hibbert A. and Berrington K.A. 1987, MNRAS 225, 377

© European Southern Observatory • Provided by the NASA Astrophysics Data System

1994A&AS..107...29S

Mohan M. and Hibbert A. 1991, Phys. Scripta 44, 158
Mohan M. and Le Dourneuf M. 1990, Phys. Rev. A 41, 2862
Mohan M., Le Dourneuf M., Hibbert A. and Burke P.G. 1990, MNRAS 243, 372
Moore C.E. 1971, Atomic Energy Levels Vol. I, NSRDS - NBS 35
Sampson D.H., Hong Lin Zhang and Fontes C. 1991, At. Data Nuc. Data Tables 48, 25
Seaton M.J. 1983, Reports on Progress in Physics 46, 167
Sharp J.M., Comer J. and Hicks P.J. 1975, J. Phys. B: At. Mol. Phys. 15, 2512
Sugar J. and Corliss C. 1977, J. Phys. Chem. Ref. Data 6, 317
Sugar J. and Corliss C. 1978, J. Phys. Chem. Ref. Data 7, 1191
Sugar J. and Corliss C. 1979, J. Phys. Chem. Ref. Data 8, 865
Sugar J. and Corliss C. 1985, J. Phys. Chem. Ref. Data 14, Suppl. 2
Vo Ky Lan 1991, private communication

Table 1. Exponents for the $\bar{3}$d pseudo orbitals, OP: Opacity Project, Hibbert & Scott 1994; Sp: spline fit to OP data*

Z	10	11	12	13	14	15	16	17	18
OP	3.381	3.985	4.532	5.079	5.624	...	6.712	...	7.798
Sp	3.437	3.986	4.530	5.084	5.625	6.168	6.710	7.254	7.799
Z	19	20	21	22	23	24	25	26	27
OP	...	8.882	...	...	...	...	...	12.131	...
Sp	8.342	8.882	9.424	9.963	10.504	11.046	11.589	12.131	12.674

* Except for $Z = 10$ for which we use the optimised value 3.43716, see discussion in Sect. 2.

Table 2. $E_{\rm th}$ and $E_{\rm ex}$ are the theoretical and experimental energies for the ^{2}P° term separation, $E_{\rm FS}$ is the experimental fine structure splitting of ^{2}P°: $f_{\rm l}$ and $f_{\rm v}$ are the oscillator strengths in the length and velocity formulations obtained with the present targets, and $f_{\rm l}^{\rm H}$, $f_{\rm v}^{\rm H}$ are those given by Mohan & Hibbert (1991). $E_{\rm L}$ is the highest impact electron energy for which a two state target representation gives valid collision data. All energies are in Rydberg units, Table 3 lists the sources of experimental data

Z	$E_{\rm th}$	$E_{\rm ex}$	$E_{\rm FS}$	$f_{\rm l}$	$f_{\rm v}$	$f_{\rm l}^{\rm H}$	$f_{\rm v}^{\rm H}$	$E_{\rm L}$
10	2.0459	1.9755	0.0071	0.086	0.095	0.091	0.095	1.70
11	2.4626	2.4057	0.0124	0.085	0.092			2.38
12	2.8797	2.8321	0.0203	0.082	0.087	0.088	0.090	3.09
13	3.2960	3.2593	0.0313	0.079	0.083			3.84
14	3.7116	3.6888	0.0465	0.076	0.078			4.69
15	4.1263	4.1217	0.0662	0.072	0.074			5.76
16	4.5401	4.5583	0.0923	0.069	0.071	0.085	0.068	6.46
17	4.9534	5.0014	0.1239	0.066	0.067	0.079	0.064	7.23
18	5.3659	5.4503	0.1645	0.063	0.064			8.08
19	5.7780	5.9055	0.2139	0.060	0.061			8.95
20	6.1896	6.3696	0.2736	0.057	0.059			9.81
21	6.6007	6.8435	0.3454	0.055	0.056			11.5
22	7.0116	7.3278	0.4300	0.053	0.054	0.059	0.050	13.5
23	7.4219	7.8254	0.5315	0.051	0.052			15.5
24	7.8322	8.3317	0.6430	0.049	0.050			17.1
25	8.2422	8.8527	0.7792	0.047	0.048			18.8
26	8.6518	9.3895	0.9350	0.045	0.046	0.046	0.045	20.9

© European Southern Observatory • Provided by the NASA Astrophysics Data System

1994A&AS..107...29S

Table 3. References giving experimental energies

Ne II	Moore 1971, Sharp et al., 1975
Na III	Martin and Zalubas 1981
Mg IV	Martin and Zalubas 1980
Al V	Martin and Zalubas 1979
Si VI	Martin and Zalubas 1983
P VII	Moore 1971
S VIII	Moore 1971
Cl IX	Deutschman and House 1966
Ar X	Deutschman and House 1966
K XI	Sugar and Corliss 1985
Ca XII	Sugar and Corliss 1979
Sc XIII	Sugar and Corliss 1985
Ti XIV	Corliss and Sugar 1979
V XV	Sugar and Corliss 1978
Cr XVI	Sugar and Corliss 1977
Mn XVII	Corliss and Sugar 1977
Fe XVIII	Corliss and Sugar 1982

Table 4. Effective quantum numbers ν relative to the $2s2p^6\ ^2S$ target term

Z	ν_{thr}	ν(3s)	ν(3d)	ν(3p)	ν_{ex}(3p)
10	0.71	1.749	2.691	2.167	2.156
12	1.78	2.166	2.959	2.444	...
14	2.60	2.384	2.933	...	...
16	3.28	2.506	2.943	2.653	2.642
18	3.86	2.577	2.941	2.705	...
20	4.36	2.635	2.928	2.745	2.743
22	4.82	2.680	2.939	2.775	2.768
24	5.20	2.713	2.939	2.799	2.792
26	5.55	2.740	2.940	2.818	2.818

Table 5. Effective collision strengths $\Upsilon(^2P^o_{3/2} - ^2P^o_{1/2})$ for F-like ions T is the temperature in Kelvin. The tabulation is restricted to temparatures at which the present calculations are considered reliable. See Table 6 for ions that present special problems

$\log T$	Z=10	Z=11	Z=12	Z=13	Z=14	Z=15	
3.00	.272	.350	.356	.381	.309	...	
3.25	.273	.350	.356	.386	.308	.512	
3.50	.274	.350	.356	.403	.305	.449	
3.75	.278	.352	.356	.450	.302	.388	
4.00	.283	.354	.357	.506	.299	.336	
4.25	.294	.357	.358	.524	.299	.295	
4.50	.311	.364	.363	.502	.321	.267	
4.75	.338	.376	.378	.474	.373	.256	
5.00	.377	.399	.403	.464	.418	.267	
5.25	...	...	.425	.459	.430	.288	
$\log T$	Z=16	Z=17	Z=19	Z=20	Z=21	Z=23	Z=24
3.50	.192	.169	.111	.100	...	...	...
3.75	.192	.169	.111	.100	...	...	...
4.00	.192	.171	.111	.100	.113	...	.059
4.25	.196	.182	.111	.101	.131	...	.059
4.50	.209	.205	.112	.104	.145	.070	.059
4.75	.234	.245	.118	.118	.165	.069	.061
5.00	.267	.279	.134	.143	.182	.076	.072
5.25	.291	.289	.157	.164	.185	.093	.090
5.50	.291	.277	.172	.172	.177	.109	.105
5.75	...	...	...	.164	.159	.112	.110

© European Southern Observatory • Provided by the NASA Astrophysics Data System

1994A&AS..107...29S

Table 6. Calculated and adjusted effective collision strenghts $\Upsilon(^2P^o_{3/2} - ^2P^o_{1/2})$ for "problem" ions, Υ are calculated as for Table 5, Υ_a are obtained as discussed in Sect. 5, Υ_{BP} are results of a relativistic calculation in the Breit-Pauli approximation

	Z=18		Z=22		Z=25		Z=26		
$\log T$	Υ	Υ_a	Υ	Υ_a	Υ	Υ_a	Υ	Υ_a	Υ_{BP}
3.50	.186	1.03	...	...	...	...	...	...	.064
3.75	.242	1.28	.081	.544	.054	.054	.049	.052	.062
4.00	.387	1.26	.091	.610	.054	.055	.050	.055	.062
4.25	.532	1.07	.135	.605	.054	.056	.050	.069	.071
4.50	.573	.837	.212	.550	.055	.064	.055	.099	.094
4.75	.514	.622	.260	.447	.061	.083	.071	.132	.127
5.00	.421	.459	.254	.338	.077	.106	.093	.143	.143
5.25	.344	.357	.222	.258	.096	.120	.107	.136	.138
5.50	.288	.292	.191	.205	.107	.123	.109	.124	.125
5.75	...	...	.165	.166	.107	.115	.104	.110	.110
6.00	...	...	...	...	.095	.099	.091	.093	.092

Table 7. Comparison of collision strengths calculated with and without relativistic effects RDW: relativistic distorted wave by Sampson et al. (1991); IP: Iron Project, present work

Z	E	Ω_{RDW}	Ω_{IP}
22	1.88	0.070	0.077
	9.41	0.062	0.063
26	2.99	0.044	0.043
	14.95	0.039	0.040

© European Southern Observatory • Provided by the NASA Astrophysics Data System